Conference Paper, Published Version

Angelotti, Natalia; Vinçon-Leite, Brigitte; Carmigniani, Rémi

Hydrodynamic modelling for early warning of sanitary risks in open swimming waters

Hydrodynamic modelling for early warning of sanitary risks in open swimming waters

Natalia Angelotti *(1)*, Brigitte Vinçon-Leite *(1)*
(1) LEESU
Ecole des Ponts ParisTech, UPEC
Champs-sur-Marne, France
natalia.angelotti-de-ponte-rodrigues@enpc.fr

Rémi Carmigniani *(2)*
(2): LHSV
ENPC, Cerema, EDF R&D
Chatou, France

***Abstract*— Swimming in open water involves sanitary risks related to the presence of pathogenic microorganisms. To ensure the safety of bathers, a regulatory monitoring in the bathing area, based on faecal indicator bacteria (FIB), is required. Analysis of FIB concentrations can take more than 10 hours with *in situ* devices and more than 24 hours in the laboratory. Hence monitoring and forecasting of the sanitary conditions in urban bathing sites are essential for decision-making on their possible closure and its duration.**

In this paper, TELEMAC-3D hydrodynamic model was used to compute the time and space distribution of water temperature, velocity and contaminant tracers considering hydro-meteorological conditions that can cause noticeable changes on the transfer time of the contaminant to the bathing area.

The study site, La Villette, is an urban canal-basin system with a bathing area, located in Paris. The objectives focus on (i) how thermal stratification affects the transfer time of upstream contamination to the bathing area; (ii) the use of conductivity to track water quality changes after a storm event and (iii) the simulation of conductivity variation.

I. INTRODUCTION

In urban areas, swimming in open water has been increasingly popular, especially in large European cities. However, the bathers can be exposed to infectious diseases caused by pathogens from faecal contamination. To avoid this, the European regulation (bathing water directive 2006/7/EC [1]) requires the implementation of a sanitary control. The regulatory indicators of pathogenic microorganisms are faecal indicator bacteria (FIB). They include *Escherichia coli* (*E. coli*), a coliform bacteria whose concentration analysis can take more than 10 hours with *in situ* devices ([2], [3]) and more than 24 hours in the laboratory [4].

To anticipate possible sanitary risks, the microbiological monitoring can be performed upstream of the bathing area. Considering the transfer time from the measuring point to the bathing area and the delay to obtain the analysis results, the information about the water quality in the bathing area can be available in due time. In addition, a hydrodynamic model can be used for computing the transfer time between the sampling point and the bathing area.

Hydro-meteorological conditions may impact the transfer time, such as flowrate variations and thermal stratification. Vertical thermal stratification causes differences in the flow velocity with depth. Therefore, the arrival time and the duration of the contamination can vary with depth in the bathing area.

On the other hand, an indicator related to faecal contamination and available in real-time would also be very beneficial for decision making about a possible closure or re-opening of the bathing area. After heavy rainfall episodes, due to stormwater network discharge and runoff on contaminated surface and, faecal contamination is observed in urban water bodies. Conductivity is one of the variables that shows good correlation with stormwater discharge, and is possibly able to track faecal contamination ([5]–[7]).

We addressed these issues in the study site of La Villette in Paris. As part of the Paris-Plage summer program, a bathing area has been open in La Villette basin since 2017. Very appreciated by the public, it received around 70 000 bathers in July-August 2019 [8].

The first objective of the study was to investigate how the thermal stratification modifies the transfer time of a microbiological contamination originated from upstream. The first results presented here relate to the contaminant transport during a hot weather episode. Then, after confirming that continuous monitoring of conductivity, upstream and in the bathing area, could track the water quality changes after a heavy rainfall episode, the second objective was to simulate the conductivity variation from upstream to the bathing area. We used the TELEMAC-3D hydrodynamic model to compute the time and space distribution of water temperature, velocity, and contamination tracer. Time series of conductivity were measured with *in situ* sensors installed upstream and at the bathing area.

II. STUDY SITE AND FIELD DATA

The study site, La Villette, is located in the north-east of Paris. It is an urban water body with recreational activities such as boat navigation and the opening of a free bathing area during summer.

The upstream part of La Villette system corresponds to a canal of 25 m wide and 800 m long. Then, it widens to 75 m wide, forming a basin of 700 m long, where the bathing area is located (Fig. 1) [9]. The whole system has a total extension of 1500 m and approximately 3 m of depth. The average annual water flow is 2.7 m^3/s.

At the outlet of the system, a navigation lock towards the St-Martin canal works from 09h00 to 19h00. Additionally, a

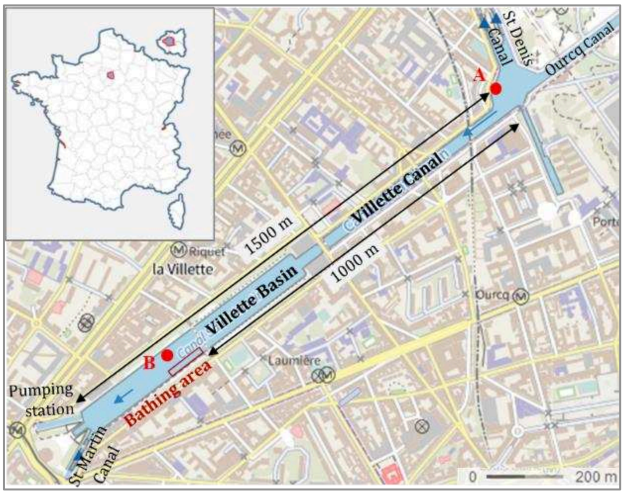

Figure 1: Location of La Villette system and the measurement points A and B (red dots)

water pumping station derives part of the volume to Paris non-drinkable water network.

The monitoring system has two points of measurements. Point A is located at the inlet of the canal, 1000 m upstream of the bathing area. Point B is located downstream, next to the bathing area, at the right bank of the basin (Fig. 1). Both points are equipped with sensors of water temperature and conductivity measured at a 10 min time step. Water temperature has been measured at three depths (0.5 m, 1.2 m, 2.0 m) and conductivity at 1.2 m depth.

III. NUMERICAL MODEL

The numerical simulations were done with TELEMAC-3D (version 8.0). The atmosphere-water heat exchanges were done with the WAQTEL module, where the thermal process was activated. The data pre-processing was carried out with BlueKenue 64 v3.3.4 and the post-processing with MATLAB R2020b.

A. Modelling domain

The model domain goes from the canal round-about at upstream to the end of the basin area at downstream. A triangulated mesh (Fig. 2) was created using the data of a bathymetry survey at 6 section profiles [10].

The 3D grid has a total of 10 layers, with approximately 0.30 m of depth. Each layer has 3185 nodes and 5680 elements. The average edge length is of approximately five meters.

The simulation results of layers 2 (bottom), 5 (middle), and 8 (surface) are compared with the field data at 2.0 m, 1.2 m, and 0.5 m, respectively.

B. Hydrodynamic model

The simulated variables are the free surface elevation, water temperature, water velocity and an indicator of microbiological quality. In alignment with the European regulation, the faecal indicator bacteria "coliforms" was selected. Water temperature was considered as an active tracer and microbiological indicator as a passive tracer [11].

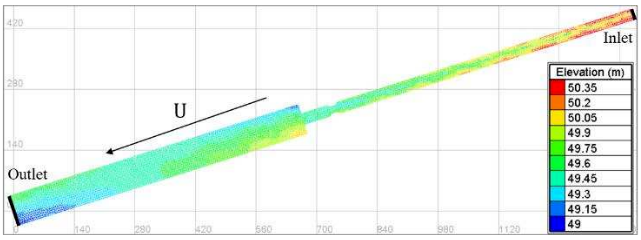

Figure 2: Mesh of the bottom layer of La Villette system

The model was set-up to consider the heat exchange between the atmosphere and the water, through the WAQTEL module.

The water density was expressed as a function of water temperature (1).

$$\rho = \rho_{ref}\left[1 - T\left(T - T_{ref}\right)^2 10^{-6}\right] \quad (1)$$

Where ρ is water density [kg/m³], ρ_{ref} is the reference density (999.972 kg/m³) at the reference water temperature T_{ref} = 4 °C, and T is the water temperature [°C].

The solar radiation attenuation in the water column is calculated according to the Beer-Lambert equation where the extinction coefficient is derived from the field data of Secchi depth [12].

The Strickler law was used for the bottom friction with the default coefficient of 60 $m^{1/3}/s$. The horizontal turbulence model considers a constant viscosity with a coefficient for diffusion of velocities of 0.1 m²/s. The adopted vertical turbulence model was the Nezu and Nakagawa mixing length (2). All the parameters have the default values.

$$L_m = \kappa z\sqrt{1 - \frac{z}{h}} \quad (2)$$

Where L_m is the mixing length, κ is the von Kármán constant (0.41), z is the distance to the bed [m] and h is the water depth [m].

The upstream boundary condition is defined as an open boundary with prescribed flowrate and tracer values. The downstream open boundary is defined with prescribed water elevation and free tracer values. The lateral boundaries are defined as a solid wall.

The input data include the flowrate and water temperature at the upstream boundary. For the heat exchange with the atmosphere, meteorological data (wind speed and direction, air temperature, atmospheric pressure, relative humidity, nebulosity, and rainfall) are also required. The meteorological data are obtained from the Orly Météo-France station. The input upstream water temperature and conductivity are measured at point A. The flowrates are calculated from the total daily volumes provided by the Service des Canaux de la Ville de Paris.

The time-step of the model computation is of 20 s. The results are given in time-step of 10 min.

C. Simulation periods

Two periods were simulated. The first one in August 2020 corresponds to a high temperature episode, to analyse the thermal stratification impact on the distribution of velocity and of the microbiological indicator, "coliforms". The latest was considered as a passive tracer in order to disentangle the effect of the water column stratification from any other biogeochemical process.

The second period, in June 2021, includes a heavy rainfall episode. On this period, the conductivity evolution, which is assumed to be a proxy of the water quality change due to the rainfall event, was simulated.

IV. Results and Discussion

A. Simulation from the 7th to the 12th of August 2020: hot weather period

The first simulated period is from 07/08/2020 to 12/08/2020 (5 days). In addition to water temperature and velocity, the variable "coliforms" was simulated as a passive tracer. It was prescribed as a step input of 1000 MPN/100mL (MPN, Most Probable Number per 100 mL), uniformly distributed in the inlet water column. It lasts for 48 hours, from 08/08/2020 to 10/08/2020. Generally, in the equation of coliforms evolution, the bacterial decrease is represented by an exponential term using a decay rate, which depends on water temperature, light intensity, and salinity [13-15]. Here, in order to assess the single effect of thermal stratification, the decay rate was set to 0. The Secchi depth is 0.9 m.

The water column is stratified during the day and mixes at night (Fig. 3). The simulated and the field data of water temperatures range from 22.8 to 26.3°C.

The simulated temperatures are close to the measured data (RMSE=0.36°C at the surface, 0.35°C at the middle and 0.41°C at the bottom). A good agreement is obtained between field data and model results: $R^2 = 0.84$ at the surface, $R^2 = 0.83$ at the middle and $R^2=0.77$ at the bottom. The maximum differences between the results and the field data are of 0.84°C at the sub-surface, 0.87°C at the middle, and 1.08°C at the bottom.

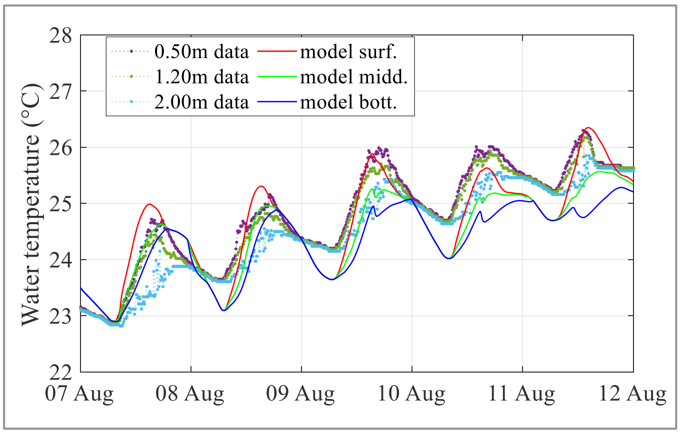

Figure 3: Measured and simulated water temperature at three depths at point B, from 07 to 12/08/2020.

The model slightly underestimates the field data by 0.6% at surface, 1% at the middle and 0.8% at the bottom.

The maximum temperature difference between the surface and bottom layers (ΔTw) can be considered as an indicator of the stratification intensity. It ranges from 0.85°C to 1.35°C for the field data and from 0.95°C to 1.6°C for the simulation results (Fig. 4). The stratification starts at the same time for both field data and model results. However, on the first three days of simulation, the mixing of the water column in the night occurs earlier in the model, 4.5 h to 7 h before the measured data.

The longitudinal current velocity (U-axis, positive towards downstream) and the coliforms concentration at point B, in the surface, middle and bottom layers are presented on Fig. 5.

At the surface, the longitudinal velocities vary from -0.03 m/s to 0.05 m/s. At the bottom, they vary from -0.03 m/s to 0.03 m/s. The velocity range of the middle layer is from 0 to 0.02 m/s, with a mean of 0.01 m/s.

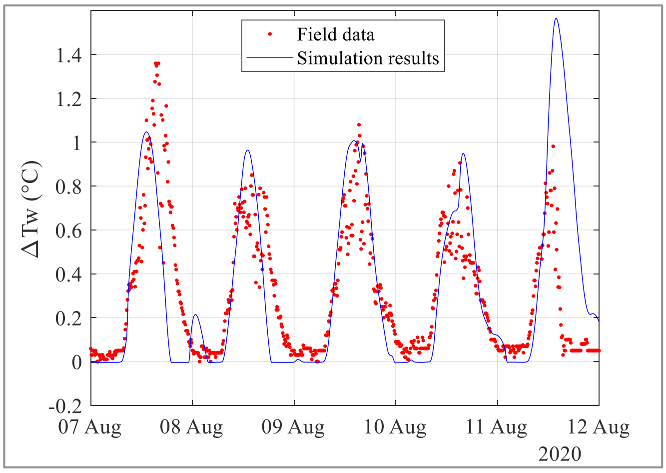

Figure 4: Difference between surface and bottom temperatures, ΔTw (field data: red, simulation results: blue), at point B, from 07 to 12/08/2020.

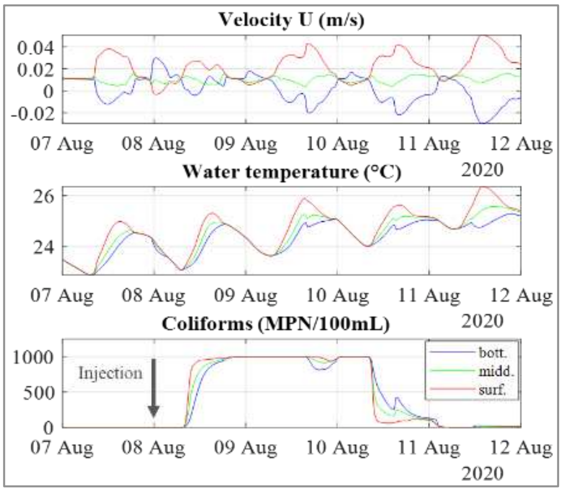

Figure 5: Simulation results of longitudinal velocity (U-axis), water temperature and coliforms concentration at point B, from 07 to 12/08/2020.

The difference between the surface and the bottom velocities is the largest when the water column is stratified, reaching up to 0.08 m/s. A return flow is then observed in the bottom layer. The difference in flow direction between the surface and the bottom layers is due to the thermal stratification on the water column, leading to vertical density gradient. In the case of constant density fluid simulations, these negative velocities at the bottom are not observed.

The arrival time of the coliforms at point B is different at the three depths. The maximum concentration is first reached in the surface layer. The transfer time in the surface layer is 13.3h, in the middle layer is 15.5 h, and at the bottom is 18.7 h.

The decrease of coliforms concentration starts on 10/08/2020 around 08:00 for the three depths. However, the decrease is faster in the surface layer. After 2 h, the surface concentration is around 130 MPN/100mL, and the bottom coliforms is 660 MPN/100mL.The bottom layer takes almost 15h to reach a concentration around 130 MPN/100mL.

B. *Simulation from the 1st to the 10th of June 2021: heavy rainfall event*

The second simulated period goes from 01/06/2021 to 10/06/2021 (9 days). A rainfall of more than 20 mm in one hour took place on 04/06/2021 at 08h00. Conductivity, considered as an indicator of the water quality, was simulated as a passive tracer. For this period, the Secchi depth is 1.5 m.

The field water temperature ranges from 18.2°C to 22.0°C (Fig. 6). The simulation results range from 18.1°C and 20.9°C. The performance indicators (RMSE and R^2) indicate a good agreement between field data and model results: at the surface $R^2 = 0.76$ and RMSE = 0.32°C, at the middle $R^2 = 0.73$ and RMSE = 0.33°C, at the bottom $R^2 = 0.75$ and RMSE = 0.30°C.

The model slightly underestimates the measured temperature, having a maximum difference of around 1.3 °C. The underestimation is of 2.2 % at the sub-surface, 2.8% at the middle, and 2.3% the bottom.

During the simulated period, the water column was stratified during the day and mixed at night. However, after the rainfall event, the water temperature decreased, and the water column remained mixed for the entire day of 05/08/2021.

The stratification decreased during the first four days of the simulation, disappears on 5 June, and occurs again on the four last days (Fig. 7). The model correctly reproduces the mixing on 5 June and the increase of stratification during the last days of the simulation.

The simulation results of longitudinal current velocity (U), water temperature and conductivity in the surface, middle and bottom layers at point B are presented on Fig. 8. The velocities range from -0.03 m/s to 0.04 m/s. The surface layer has the higher velocities. As on the previous simulated period, the velocity is negative in the bottom layer.

At the beginning of the simulated period, the conductivity is uniform in the water column. Following the rainfall event, a continuous decrease of the conductivity was observed upstream (Fig. 9). It dropped from around 790 to 610 µS/cm in 3 days. Afterwards, the conductivity increased continuously for also 3 days.

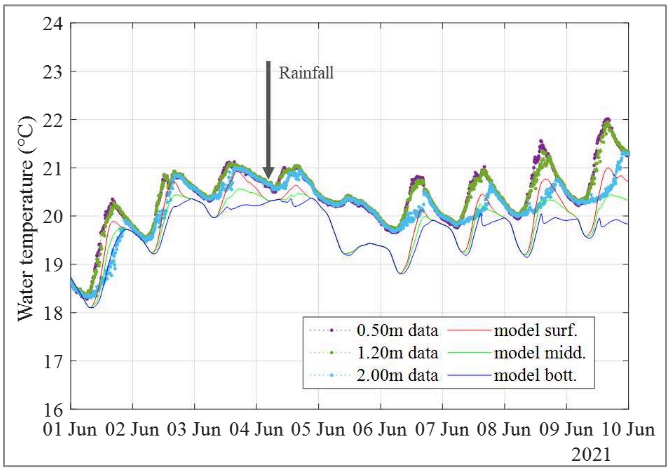

Figure 6: Water temperature at three depths from the simulation results and measured at point B.

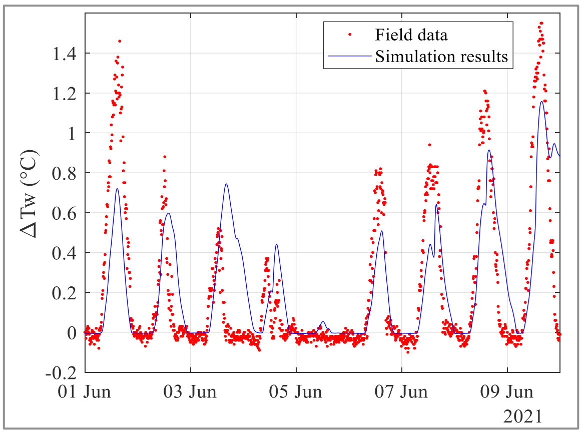

Figure 7: Difference between surface and bottom temperatures, ΔTw (field data: red, simulation results: blue), at point B from the 01 to 10/06/2020.

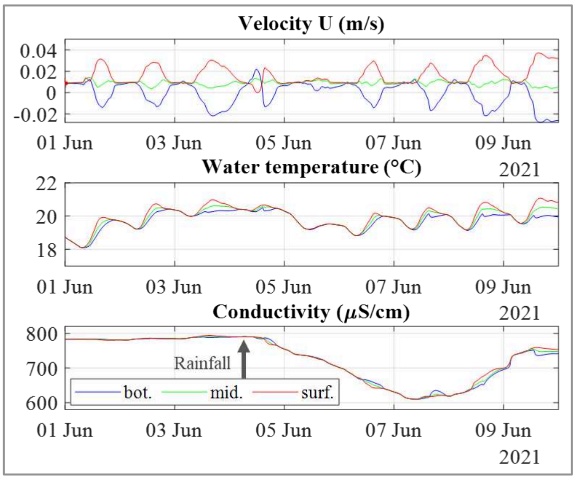

Figure 8: Simulation results of longitudinal velocity (U-axis), water temperature and conductivity, at point B from 01 to 10/06/2021.

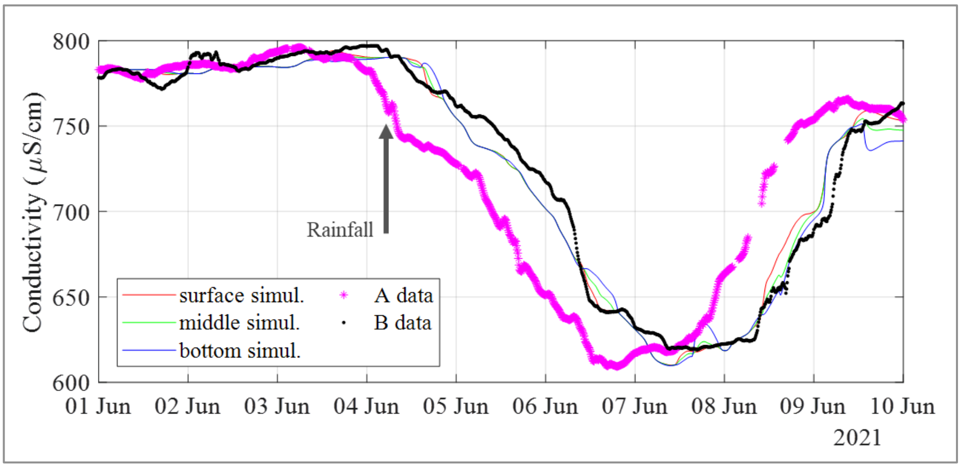

Figure 9: Conductivity measurements at points A (*) and B (·) and simulation results for three depths at point B, from 01 to 10/06/2021.

The conductivity variation observed downstream was well reproduced (Fig. 9). The simulation results and the measured conductivity show a good agreement, $R^2 = 0.98$ and RMSE = 9.0 µS/cm.

On 04/06/2021, a value of around 790 µS/cm is observed at both points (A and B). The minimum value of 610 µS/cm is observed upstream (point A) on 06/06/2021, at 19:10. Downstream, at point B, this minimum value is observed on 07/06/2021, at 11:50 and at 9:50 through the model results.

The transfer time between points A and B (1000 m) can be estimated using the time-lag between the same conductivity values at both points.

The transfer time and the mean velocity according to the simulation results and to the field data are presented in Tab. 1. The values estimated from the model results are close to the field data. The model anticipates by a few hours the arrival of the upstream water.

TABLE 1 TRANSFER TIME AND MEAN VELOCITY ESTIMATION AT MID-DEPTH (1.20 M)

Conductivity	**Date (2021)**			**Transfer time (hh:mm)**		**Mean velocity (cm/s)**	
	Point A	***Point B***	***Simul. result***	***Simul.***	***Field data***	***Simul.***	***Field data***
750 µS/cm	04/06 08:00	05/06 10:00	05/06 01:50	17:50	26:00	1.6	1.1
700 µS/cm	05/06 09:40	06/06 06:20	06/06 00:40	15:00	20:40	1.9	1.3
650 µS/cm	06/06 01:30	06/06 11:30	06/06 15:10	13:40	10:00	2.0	2.8
610 µS/cm	06/06 11:40	07/06 08:40	07/06 03:30	15:50	21:00	1.8	1.3

V. CONCLUSIONS AND PERSPECTIVES

TELEMAC-3D has been applied for microbiological modelling in some studies (*e.g.* [13], [14]) but generally in coastal study sites where the thermal stratification is negligible.

In this study, TELEMAC-3D hydrodynamic model was used to compute the time and space distributions of microbiological contaminant indicators in a thermally stratified water body.

The thermal stratification of the water column during the day was correctly captured by the model as well as the overnight mixing. In particular, the temperature difference between the surface and the bottom of the water column was well reproduced.

During the periods of thermal stratification, the longitudinal velocity is the surface layer is faster. This affects the transfer time of the tracers, depending on the depth.

Regarding the simulated period of June 2021, when a heavy rainfall occurred at the study site and in the upstream catchment, a continuous and strong decrease of the conductivity was observed at upstream and at downstream with a few hour time-lag. This confirms that conductivity can be used to track the water quality changes after a heavy rainfall episode. The simulation results with the conductivity as a passive tracer showed a good agreement with the field data.

In conclusion, the thermal stratification observed in the field data during hot weather periods could be correctly simulated by TELEMAC-3D. It can be used to assess the transfer time of a microbiological contamination measured upstream to the bathing area of La Villette. The model was able to correctly simulate the conductivity evolution to track water quality changes after a rainfall episode in the catchment.

ACKNOWLEDGEMENT

This work is part of the OPUR project. We express our gratitude to our colleagues from ENPC/LEESU particularly for the design and implementation of the system: Philippe Dubois and Duong Tang, and for the field campaigns: Mohamed Saad, Amanda Tolentino Mendes, Guilherme Calabro and Francesco Piccioni.

The authors would like to thank Thierry Mareschal, from the Service des Canaux de la Ville de Paris, for his help and availability. We would also like to thank Yael (responsible of Paris base), César (manager of Paris base) and all the crew from Marin d'Eau Douce for their support for the field work.

REFERENCES

[1] EU, 'Directive 2006/7/EC of the European Parliament and of the Council of 15 February 2006 concerning the management of bathing water quality and repealing Directive 76/160/EEC'. Feb. 15, 2006. Accessed: Nov. 16, 2020. [Online]. Available: https://eur-lex.europa.eu/legal-content/GA/TXT/?uri=CELEX:32006L0007

[2] S. Guérin-Rechdaoui *et al.*, 'Mesure de la qualité microbiologique des eaux de surface par le Système ALERT de fluidion. Présentation des essais laboratoire sur la matrice "eau de Seine"', *EIN*, no. 399, pp. 89–95, 2017.

[3] D. E. Angelescu *et al.*, 'Autonomous system for rapid field quantification of Escherichia coli in surface waters', *J. Appl. Microbiol.*, vol. 126, no. 1, pp. 332–343, Jan. 2019, doi: 10.1111/jam.14066.

[4] A. Tiwari, S. I. Niemelä, A. Vepsäläinen, J. Rapala, S. Kalso, and T. Pitkänen, 'Comparison of Colilert-18 with miniaturised most probable number method for monitoring of Escherichia coli in bathing water', *Journal of Water and Health*, vol. 14, no. 1, pp. 121–131, Feb. 2016, doi: 10.2166/wh.2015.071.

[5] S. Frank, N. Goeppert, and N. Goldscheider, 'Fluorescence-based multi-parameter approach to characterize dynamics of organic carbon, faecal bacteria and particles at alpine karst springs', *Science of The Total Environment*, vol. 615, pp. 1446–1459, Feb. 2018, doi: 10.1016/j.scitotenv.2017.09.095.

[6] D. E. Nnane, J. E. Ebdon, and H. D. Taylor, 'Integrated analysis of water quality parameters for cost-effective faecal pollution management in river catchments', *Water Research*, vol. 45, no. 6, pp. 2235–2246, Mar. 2011, doi: 10.1016/j.watres.2011.01.018.

[7] M. Seo, H. Lee, and Y. Kim, 'Relationship between Coliform Bacteria and Water Quality Factors at Weir Stations in the Nakdong River, South Korea', *Water*, vol. 11, no. 6, p. 1171, Jun. 2019, doi: 10.3390/w11061171.

[8] Seine-Saint-Denis Tourisme, 'Bilan d'activité 2019 et perspectives d'action pour 2020', Agence de développement touristique, 2019. Accessed: Mar. 12, 2021. [Online]. Available: https://ressources.seinesaintdenis.fr/IMG/pdf/2._bilan_activites_organismes_exterieurs_2019_-_annexe_partie2.pdf

[9] SAFEGE, 'Elaboration d'un profil de baignade pour une baignade publique sur le bassin de la Villette à Paris. Rapport de phase 1: Etats des lieux'. Mairie de Paris-Suez, 2017.

[10] F. Bezerra *et al.*, 'Open-water swimming in urban areas: How a three-dimensional hydrodynamic model can help in the microbiological contamination monitoring?', presented at the Novatech Urban Water - Planning and technologies for sustainable management Novatech, Lyon, 2019. [Online]. Available: http://www.novatech.graie.org/documents/auteurs/2B4P-273VIN.pdf

[11] EDF R&D and Telemac3d consortium, *TELEMAC-3D User Manual, Version 8.0*. TELEMAC-MASCARET, 2018.

[12] S. B. Idso and R. G. Gilbert, 'On the Universality of the Poole and Atkins Secchi Disk-Light Extinction Equation', *Journal of Applied Ecology*, vol. 11, no. 1, pp. 399–401, 1974, doi: 10.2307/2402029.

[13] J. King, R. Ahmadian, and R. A. Falconer, 'Hydro-epidemiological modelling of bacterial transport and decay in nearshore coastal waters', *Water Research*, vol. 196, p. 117049, May 2021, doi: 10.1016/j.watres.2021.117049.

[14] J. Dugor, J. Baills, and D. Rihouey, 'Numerical modelling of bacteriologic impacts in the Laïta estuary (France)', presented at the Telemac User Conference 2019 (TUC2019), Toulouse, Jan. 17, 2020. doi: 10.5281/zenodo.3611538.

[15] L. Selméus, 'Dynamic modelling of bathing water quality with biodegradation of Escherichia coli in TELEMAC-3D', Lund University, 2018.